AD-A049 876 NAVAL POSTGRADUATE SCHOOL MONTEREY CALIF F/G 1/3
PROGRESS REPORT ON AIRCRAFT FATIGUE STUDIES.(U)
SEP 77 G H LINDSEY
UNCLASSIFIED NPS-67LI77091 NL

| OF |
AD
A049 876

END
DATE
FILMED
3-78
DDC

NPS-67Li77091

NAVAL POSTGRADUATE SCHOOL

Monterey, California

PROGRESS REPORT ON
AIRCRAFT FATIGUE STUDIES

BY

GERALD H. LINDSEY

September 1977

Prepared for:
Naval Air Systems Command
Code AIR-803
Washington, DC 20361

NAVAL POSTGRADUATE SCHOOL

Monterey, California

Rear Admiral I. W. Linder
Superintendent

Jack R. Borsting
Provost

The work reported herein was supported by Naval Air Systems Command, Washington, DC.

This report was prepared by:

GERALD H. LINDSEY

Reviewed by:

R. W. BELL, Chairman
Department of Aeronautics

R. R. FOSSUM
Dean of Research

UNCLASSIFIED

SECURITY CLASSIFICATION OF THIS PAGE (When Data Entered)

REPORT DOCUMENTATION PAGE	READ INSTRUCTIONS BEFORE COMPLETING FORM
1. REPORT NUMBER: NPS-67Li77091	2. GOVT ACCESSION NO. / 3. RECIPIENT'S CATALOG NUMBER
4. TITLE (and Subtitle): Progress Report on Aircraft Fatigue Studies.	5. TYPE OF REPORT & PERIOD COVERED: Interim Report, 1 July 1976–30 September 1977
	PERFORMING ORG. REPORT NUMBER
7. AUTHOR(s): Gerald H. Lindsey	8. CONTRACT OR GRANT NUMBER(s): N00019-77-WR-71012
9. PERFORMING ORGANIZATION NAME AND ADDRESS: Naval Postgraduate School, Monterey, CA 93940	10. PROGRAM ELEMENT, PROJECT, TASK AREA & WORK UNIT NUMBERS: LPN A3203200/186A/7R023-00-000
11. CONTROLLING OFFICE NAME AND ADDRESS: Naval Air Systems Command, Code AIR-803, Washington, DC 20361	12. REPORT DATE: September 30, 1977
	13. NUMBER OF PAGES: 31
14. MONITORING AGENCY NAME & ADDRESS (if different from Controlling Office): 35p.	15. SECURITY CLASS. (of this report): UNCLASSIFIED
	15a. DECLASSIFICATION/DOWNGRADING SCHEDULE

16. DISTRIBUTION STATEMENT (of this Report)

Approved fpr public release; distribution unlimited

17. DISTRIBUTION STATEMENT (of the abstract entered in Block 20, if different from Report)

18. SUPPLEMENTARY NOTES

19. KEY WORDS (Continue on reverse side if necessary and identify by block number)

Aircraft Fatigue
Cumulative Damage
Neuber's Equation
Residual Stress

20. ABSTRACT (Continue on reverse side if necessary and identify by block number)

This report summarizes a year of research activity on aircraft fatigue in three areas: (1) The influence of minimum load levels, ground loads, order of loading and counting method on the damage calculation, (2) The method of calculating local stress in the plastic range at the stress concentration site from the recorded in-flight strain monitor and (3) The measurement of relaxation of residual stresses after they are produced locally at the point of stress concentration. Substantial progress was made in all three areas and especially the first two.

DD FORM 1 JAN 73 1473 (Page 1) EDITION OF 1 NOV 65 IS OBSOLETE S/N 0102-014-6601

251 450

SECURITY CLASSIFICATION OF THIS PAGE (When Data Entered)

ABSTRACT

This report summarizes a year of research activity on aircraft fatigue in three areas: (1) The influence of minimum load levels, ground loads, order of loading and counting method on the damage calculation, (2) The method of calculating local stress in the plastic range at the stress concentration site from the recorded in-flight strain monitor and (3) The measurement of relaxation of residual stresses after they are produced locally at the point of stress concentration. Substantial progress was made in all three areas and especially the first two.

TABLE OF CONTENTS

I. INTRODUCTION AND BACKGROUND

Early Developments

Commencing three years ago, a feasibility study was undertaken to determine if an effective aircraft fatigue monitoring instrument could be conceived on the basis of microprocessors. The goal was to design a small, lightweight package, which could record maximum and minimum loads sequentially in a form conducive to automated data processing. The first unit was designed and fabricated by LT David Vidrine (1) and LT James Sturgis (2). This first prototype was physically larger than would have resulted for an optimum design solely for fatigue monitoring in order to give it testing, check-out, and development capability. It was built around the Intel 8008 CPU chip, and had 16 channel capacity via a multiplexer. It digitized the incoming load information from strain gages, accelerometers, or other transducers and then searched these signals for maxima and mimima. Upon finding them, the digital value of each extremum point was stored in memory in chronological order until the memory was filled, at which point, the microprocessor caused the tape recorder to be activated, and the memory to be transferred to the tape cassette.

This unit was laboratory tested with sinusoidal signals from signal generators with results as shown in Fig. 1. After success was obtained with known signals, the unit was flight tested in an NPS leased Cessna 310. Typical results are shown in Figure 2.

Second Prototype

In those budding days of microprocessors, the state of the art was advancing rapidly as it is today, and by the time the first prototype was built, new developments had been perfected. LT Wesley Stanfield (3) began work on a second prototype that was directed toward flight test in a high

performance aircraft. It was based on the 8008 CPU, but incorporated advancements in programming capability and reduction in the physical size of the components. It was designed with 8 channel capacity and had the physical dimensions shown in Figure 3. The final version of the software was generated by LT Charles Butler (4), who also generated the programs for data reduction from the instrument through a Hewlitt Packard 9830, desk-top computer.

This second prototye was successfully laboratory tested and demonstrated for Dr. David Weiss of the Naval Air Development Center (NADC). The instrument was able to take data from signal generators up to $5H^2$, pick out maxima and minima and record them on tape. Using the HP 9830, the voltage of the maxima and minima are listed in tabular form in chronological sequence.

Final Results

This concluded the feasibility study at NPS, and the Naval Air Systems Command, through Bob Weinberger, adopted the concept of an in-flight microprocessor instrument to monitor fatigue as well as other flight and engine parameters. The F-18 was designated as the first Navy aircraft to incorporate the concept, and all future aircraft will use state-of-the-art versions of this fatigue monitoring concept.

The second prototype instrument was then to be transitioned to Dr. Weiss at NADC for further experimentation while new prototypes were designed and packaged to meet military specifications. A malfunction in the analog to digital conversion unit was experienced at this time. Steps taken to correct it finally required a new unit from an alternate manufacturer, which in turn precipitated changes in the wiring and associated changes in the software. In the meantime, further developments in microprocessor technology have made significant investments of time in the second prototype unit unwarranted.

Future Possibilities

In the original prototyping, a tape recorder was used as the final reservoir of the data. This was a temporary arrangement because of the limited conditions under which successful tape recorder operations can occur. Large temperature and humidity variations can cause the capstans to freeze, and recording in a high g environment may not be reliable at all; however, there is an alternative emerging.

Two specific possibilities have recently come forth: one is a CMOS storage cell, which requires so little power that small batteries can sustain them into the time ranges of weeks that would be needed for actual operations. The second is Texas Instrument's bubble memory, which at this time is not completely reliable but which has promise to fill the needs of the system in the not too distant future by providing large quantities of nonvolatile memory capacity.

II. DAMAGE CALCULATION

In light of the Navy commitment to employ microprocessor units as fatigue monitors, it now becomes appropriate to look forward to the type of data that will be available from them and how it can be used to calculate fatigue damage.

Two General Approaches

The Navy for many years has used a cumulative damage approach to fatigue, based upon Miner's Law or some variation of it, which has now been developed into a rather complex calculation that considers various methods of counting the cycles, plastic flow around the point of stress concentration, residual stresses and their relaxation, etc. On the other hand the Air Force is pursuing fatigue calculations based upon crack propagation. An initial flaw of .050 in. is assummed to exist at each critical stress riser location, and the number of cycles required to grow it to a critical size constitutes the fatigue life.

Two large computer programs have been imported and made operational on the NPS IBM 360. Potter's (5) cumulative damage program uses Miner's Law and is presently operational. Engels (6) program, "Cracks II," employ the crack propagation method and is now being checked out with example problems provided by the author. Check runs are planned in the future to give comparisons of fatigue lives for the same conditions and to investigate the affect of cycle minimums in the load spectrum. The calculations will be for an actual airplane fatigue critical point on the A-7E.

Potter Program

LT Scott Atkinson (7) has investigated the influence of counting method and type of block loading on damage. The load spectrum used in the analysis was the spectrum which is reproduced in Table I, from MIL SPEC A8866, and the

TABLE I

FREQUENCY OF MANEUVER LOADS

NUMBER OF TIMES PER THOUSAND HOURS THAT LOAD FACTOR IS EXPERIENCED

PERCENT OF MAXIMUM (POSITIVE) SYMMETRICAL LIMIT LOAD FACTOR	FLIGHT MANEUVER LOAD SPECTRUM A
35	17000
45	9500
55	6500
65	4500
75	2500
85	1360
95	440
105	150
115	40
125	16
TOTAL	42006

PERCENT OF MAXIMUM (NEGATIVE) SYMMETRICAL LIMIT LOAD FACTOR	FLIGHT MANEUVER LOAD SPECTRUM A
0	500
10	200
20	100
30	60
40	35
50	30
60	25
70	20
80	15
90	10
100	5
110	3
TOTAL	1003

loads are assumed to be applied at wing station 32 on an A-7E wing (8). Load data were input as block loads and also as single randomized cycles. The Miner's Law summation of fatigue damage for this loading spectrum is .1300 per 1000 flight hours. Results obtained using this computer program are given in Tables II, and III. It is important to notice that when fatigue damage is calculated without using the range-pair counting method, it makes only a minor difference on the total fatigue damage when the sequence of loading is changed or when negative loads are included.

Block loads were arranged in LO-HI, HI-LO, and HI-LO-HI sequences. The results indicate the LO-HI sequence to be more damaging than the HI-LO sequence, with damage due to the HI-LO-HI sequence falling between the other two block load sequences. In the HI-LO sequence the HI loads leave a local residual compressive stress in the material, and the LO loads do less damage.

In the case of randomly generated load sequences, identical starter integers were used in order to evaluate the effect on the damage of inclusion of MIL spectrum A negative loads and ground cycles. The more negative loads that are included, the worse is the fatigue damage. The increase in damage with more negative loads is caused by the negative loads decreasing the local residual compressive stress caused by positive loads into the plastic zone. This permits the local positive elastic stresses to be more damaging.

Minimum Load Levels

Including the negative values of stress resulting from landing loads, which through the range-pair counting method is tantamount to appropriately accounting for the ground-air-ground cycle, makes considerable difference in damage accumulated even for this high performance airplane. This is, of course, contrary to many statements in the literature that GAG cycles are only of significance in transport aircraft, and this conclusion is proper when

TABLE II

FATIGUE DAMAGE DUE TO POSITIVE MILSPEC A

BLOCK LOADING, NORMALIZED TO 1000 HOURS

SEQUENCE OF BLOCK LOADS	11% LIMIT LOAD MIN. USING RPCM*	11% LIMIT LOAD MIN. NOT USING RPCM*
LO-HI	.16780102	.16780108
HI-LO	.069243014	.069243014
HI-LO-HI	.10864216	.10839599

* RANGE-PAIR COUNTING METHOD

TABLE III

FATIGUE DAMAGE DUE TO MILSPEC A

RANDOMIZED LOAD INPUTS, USING RPCM, NORMALIZED TO 1000 HOURS

INTEGERS USED TO START RANDU	MINIMUM LOAD VALUES		
	11 PERCENT LIMIT LOAD	NEGATIVE MILSPEC A	GROUND CYCLES
83745,54711,54487	.039226338	.046267733	.060848035
13547,66549,7	.095124505	.085063167	.10429338
9,583,4777	.043321513	.043640956	.036781987
48621,3,491	.018672124	.034077277	.035881512
73,559,1001	.031819174	.042006299	.037130679
357,833,1	.037665060	.049336702	.050973855

residual stresses are not being accounted for. However the negative loads cause a reduction in the protective residual stress at the stress concentration site and an associated increase in damage as shown by the third column of Table III.

The entire question of minimum loads is raised at this point. Since minimum loads are not recorded at each cycle on the accelerometer counters, it has always been assumed that the minimum of each cycle was 1g., which is intuitively thought to be unrealistic. However from the data in Table III, the minimums are important and that information will be recorded and available for use from the new microprocessor fatigue monitoring instruments. In the meantime, flight testing on current aircraft with the same instruments can be used to generate a spectrum of minimum load levels for each cycle. This spectrum can then be randomized and used in the program in the same way that the 11% loads and the negative MILSPEC A loads were used in this study.

Random Load Histories

Figure 4 illustrates the pattern of the individual load randomization process and portrays the first two flight hours of the aircraft. The range of values in the columns of Table III are caused by such variations in the load randomization pattern.

The fatigue damage resulting from randomization of loads on a cycle basis, as shown in Table III, is significantly different from the damage due to the HI-LO-HI block loads illustrated in Table II, which has been accepted by many as being representative of random loading. For instance, Vought Aeronautics Division recently conducted a fatigue study using randomized flights where each flight was based on a mission profile specified by the Air Force. They found fatigue damage resulting from the randomized flights was in close agreement with fatigue damage resulting from HI-LO-Hi block loading.

Table IV has been compiled to show the influence of not using the range-pair counting method. van Dijk's (9) arguments are so compelling concerning the advisability of using the range-pair method and these results show that it should be used although it is considerably more expensive to run. The range-pair counting method relates the load sequence to the stable, cyclic, stress-strain behavior of a material by coupling up strain ranges so that each combination of half cycles will produce a complete, closed stress-strain hysteresis loop in order to be counted as a cycle.

The range-pair counting method is illustrated in Figure 5. It counts a strain range as a cycle if it can be paired with a subsequent straining of equal magnitude in the opposite direction. For a complicated load history, some of the ranges counted as cycles will be simple ranges, such as 2-3, during which the strain does not change direction, but others, such as 1-8, will be interrupted by smaller ranges, which will also be counted as cycles. In Figure 5, ranges are marked with solid lines and the paired ranges with dashed lines.

Each peak is taken in order as the initial peak of a range, except that a peak is skipped if the part of the history immediately following it has already been paired with a previously counted range. If the initial peak of a range is a minimum, a cycle is counted between this minimum and the most positive maximum which occurs before the strain becomes more negative than the initial peak of the range. For example, in Figure 5 a cycle is counted between peak 1 and peak 8, peak 8 being the most positive maximum that occurs before the strain becomes more negative than peak 1. If the initial peak of a range is a maximum, a cycle is counted between this maximum and the most negative minimum, which occurs before the strain becomes more positive than the initial peak of the range. For example, in Figure 5 a cycle is counted

between peak 2 and peak 3, peak 3 being the most negative minimum before the strain becomes more positive than peak 2. Each range that is counted is paired with the next straining of equal magnitude in the opposite direction, explaining why complete cycle rather than half cycle counts are made. For example, in Figure 5 part of the range between peaks 8 and 9 is paired with the range counted between peaks 1 and 8.

TABLE IV

FATIGUE DAMAGE DUE TO MILSPEC A RANDOMIZED LOAD

INPUTS, NOT USING RPCM, NORMALIZED TO 1000 HOURS

INTEGERS USED TO START RANDU	MINIMUM LOAD VALUES		
	11 PERCENT LIMIT LOAD	NEGATIVE MILSPEC A	GROUND CYCLES
83745,54711,54487	.040602274	.047398917	.049124956
13547,66549,7	.040137805	.047727041	.049612150
9,583,4777	.041204430	.048346408	.049540661
48621,3,491	.041160211	.049230121	.050957575
73,559,1001	.040792227	.047043338	.049311966
357,833,1	.041056350	.049220584	.050481893

III. LOCAL STRESS CALCULATION

There are two aspects of this program that require further investigation, and the first of these, local stress calculation will be discussed in this section. By local stress is meant the stress at the site of the stress concentration. The transfer function between the local stress and the far-field strain of a skin in uniaxial tension must be a function of the geometry of the notch or hole, the local strain, and the type of material.

$$\sigma = f\ (E, \rho, a, \varepsilon, s, e) \tag{1}$$

where

E = Young's Modulus

ρ = Geometric parameter - radius of curvature of the notch or hole.

a = Geometric parameter - size of the notch or hole

ε = Local strain

s = Far-field stress

e = Far-field strain

To nondimensionalize this set of variables, stress concentration factors are used. For instance any notch can be fit with an ellipse as proposed by Inglis (11), and the stress concentration factor for an ellipse in the elastic range is

$$K_t \equiv \frac{\sigma}{s} = \left[1 + 2\sqrt{\frac{a}{\rho}}\right] \tag{2}$$

Defining dimensionless ratios for local stress and strain in the plastic range in the natural way,

$$K_\sigma \equiv \frac{\sigma}{s} \qquad K_\varepsilon \equiv \frac{\varepsilon}{e} \tag{3}$$

the transfer function can be simplified to

$$K_\sigma = f\ (K_\varepsilon,\ K_T) \tag{4}$$

Neuber (12) proposed a function to describe this relationship in the form of a geometric mean of the stress and strain concentration factors.

$$K_\sigma K_\varepsilon = K_T^{\ 2} \tag{5}$$

This was evaluated on 7075-T651 experimentally by Garske (13) by using large notched plates so that strain gages could be placed at the stress concentration for reliable local strain readings. Four plates were studied with $K_T = 3.92$, 3.33, 2.51 and 1.63. Neuber's relationship was found to be in error in predicting local stresses and strains by as much as 24% in the higher plastic range in all four sheets.

From the appearance of the data in graphical plots and guided by Neuber's original proposal, a slightly generalized form of the power law was proposed.

$$K_\sigma^{\ x}\ K_\varepsilon^{\ y} = A\ K_T^{\ z} \tag{6}$$

To properly maintain the elastic limit condition where $K_\sigma = K_\varepsilon = K_T$, $A = 1$ and $z = x + y$.

$$K_\sigma^{\ x}\ K_\varepsilon^{\ y} = K_T^{\ x+y} \tag{7}$$

Without loss of generality, y can be set to one for later ease in calculation. Rearranging,

$$\left(\frac{K_\sigma}{K_T}\right)^x \left(\frac{K_\varepsilon}{K_T}\right) = 1 \tag{8}$$

A curve fit of the stress and strain concentration in the plastic range was made of the data for plate #3 for which $K_T = 2.51$. For a correlation coefficient of .90, the result was

$$\left(\frac{K_\sigma}{K_T}\right)^{1.244}\left(\frac{K_\varepsilon}{K_T}\right) = .966 \tag{9}$$

The fact that this came very close to the proper elastic limit constant of unity was very encouraging that the general form is correct. Whether there is something fundamental in the form of the equation and 1.24 should be 5/4 is not known.

It has the general appearance of an energy density, but after several attempts to derive it from fundamental principles failed, it was taken as an empirical law as it is. However to keep the appropriate and consistent elastic form, the equation should be

$$\left(\frac{K_\sigma}{K_T}\right)^{1.244}\left(\frac{K_\varepsilon}{K_T}\right) = 1 \tag{10}$$

In further calculations this equation (10) will be used.

To carry out the calculations, the stress-strain relationship was formulated from experimental data on 7075-T651 in the classical Ramburg-Osgood form by a power law curve fit of the plastic stress-strain data points.

$$\varepsilon = \left[\frac{\sigma}{10.22\text{x}10^6}\right] + \left[\frac{\sigma}{99815}\right]^{22.678} \tag{11}$$

This expression fit the nonlinear portion of the uniaxial data with a correlation coefficient of .98.

The final expression of local stress as a function of far-field strain can now be formulated from the rearranged geometric equation (10).

$$\left(\frac{\sigma}{s}\right)^{1.244}\left(\frac{\varepsilon}{e}\right) = K_T^{2.244} \tag{12}$$

Since $s = Ee$,

$$\left(\frac{\sigma}{E}\right)^{1.244}\varepsilon = (K_T e)^{2.244} \tag{13}$$

Inserting the stress-strain expression for ε,

$$\left(\frac{\sigma}{10.22\text{x}10^6}\right)^{2.244} + \left(\frac{\sigma}{1.27\text{x}10^5}\right)^{23.922} - (K_T e)^{2.244} = 0 \tag{14}$$

Solutions of this equation for stress over a range of values of far-field strains gave maximum variations of 4% from the test data for the three different K_T's tested.

With the local stress determined accurately, the residual stress can be determined accurately by assuming elastic unloading. For instance, if the fatigue monitor returned with a sequence of recorded strains as shown in Table 1, the corresponding local stresses could be calculated by the techniques that have been developed here.

TABLE I

$K_T = 1.63$

Cycle	Far-field strain	Far-field stress (psi)	Local Stress (psi)
1st Peak	.005308	54,248	77,163
1st Valley	.000000	0	- 11,260
2nd Peak	.001455	14,870	12,960
2nd Valley	.000000	0	- 11,260

The first peak local stress comes from equation (14) using the given far-field strain and K_T . The far-field stress producing it is $s = E\ (.005308) = 54,248$. The first valley stress is calculated by removing the far-field stress of 54,248 psi, which corresponds to locally removing $\Delta\sigma = K_T S = (1.63)(54,248) = 88,424$ psi. Subtracting 88,424 psi from the peak stress of 77,163 psi gives the residual stress of - 11,260 psi after the first cycle. The second cycle strain of .001455 produces a stress increase from equation (14) of 24,226 psi. However since there was a residual of - 11,260 psi, the second cycle peak stress will be 12,966 psi. Upon unloading, since there has been no plastic yielding, the structure returns to the same residual stress state as before. The first cycle yielding has been of considerable benefit in protecting the structure during the second cycle with a compressive residual stress, which reduces the fatigue damage accumulated. This can be repeated throughout a randomized or an actually recorded load history where the range-pair counting method has been incorporated.

IV. RESIDUAL STRESS RELAXATION

The second of the two aspects of the program that requires investigation is the relaxation of the residual stress created by loads into the plastic. In the true sense of the word, stress relaxation is stress decay under constant strain, but for the present the term stress relaxation will be used more loosely to mean stress reduction with time and will be descriptive of residual stress behavior with time.

When structures containing stress concentrations are loaded sufficiently to produce local plastic straining in the region of high stress, residual compressive stresses remain in that region upon unloading of the structure, as has been described. The residual stress and strain are highly localized disturbances in the elastic continuum, and since they are disturbances, they are potentially unstable. Given sufficient conditions, they will tend to be reduced and will relax toward lower values during succeeding cycles until the next overload occurs. Potter (10) has proposed that the residual stress be decomposed into an equilibrium portion and a transient portion and suggested an exponential to model the transient behavior, thinking of it as being similar to a transient in a critically damped dynamic system. The overload triggers the impulse and controls its height, and following the impulse, there is an asymptotic return to an equilibrium state. Potter's model for residual stress, σ_R, could be expressed as follows:

$$\sigma_R = \sigma_{REQ} + \sigma_{RTRANS} \tag{15}$$

In terms of the proposed exponential,

$$\sigma_R = \sigma_{REQ} + Ae^{bN} \tag{16}$$

N = Number of cycles

where it is assumed that the transient residual stress decreases with cycles

A and b are evaluated from the initial conditions and the end conditions. If $\sigma_R = \sigma_{RO}$ at $N = 0$, then

$$A = \sigma_{RO} - \sigma_{REQ} \tag{17}$$

If $N = N_{EQ}$ is the point when the transient residual stress is 90% relaxed; i.e. $\sigma_R = \sigma_R - .9\ (\sigma_{RO} - \sigma_{REQ})$

$$b = \frac{\ln 0.1}{N_{EQ}} \tag{18}$$

this gives for σ_R,

$$\sigma_R = \sigma_{REQ} + (\sigma_{RO} - \sigma_{REQ})e^{(\ln 0.1 \frac{N}{N_{EQ}})} \tag{19}$$

or

$$\sigma_R = \sigma_{REQ} + (\sigma_{RO} - \sigma_{REQ})e^{-2.3 \frac{N}{N_{EQ}}} \tag{20}$$

Experimental tests on uniaxial specimens were run by Bentley (14) to evaluate the undetermined parameters in this model and study this general behavior. The first area of interest was in the mechanism of the substructural recovery, by relaxation of the lattice structure, that accounts for the stress decay toward a stabilized stress level. Cyclic relaxation tests on 7075-T7651 into the plastic zone between fixed strain levels revealed no detectable stress relaxation. Consistently every relaxation test showed the reloading stress—strain curve rejoined at the point of departure from the original stress—strain curve for the cyclic unloading, which is evidence of zero relaxation. However, another recovery mechanism, anelastic behavior, was measured, and it was concluded that it was the primary element producing residual stress decay.

Anelastic behavior is illustrated in Figure 6, where it is seen that all of the plastic strain present at unloading is not permanent set, but some of it is recovered. After the load was removed, the ε_p continued to decrease exponen-

tially with time for periods of the order of one hour. Using the same form of the model as we did for stress,

$$\varepsilon = \varepsilon_{equil.} + \varepsilon_{transient} \tag{21}$$

and

$$\varepsilon_{trans} = (\varepsilon_p - \varepsilon_{eq})\exp(-2.303\ t/t_{eq}) \tag{22}$$

At a point of stress concentration in the structure, the material under highest stress may be thought of as a miniature uniaxial specimen as shown in Figure 7. After plastic straining at this location, the specimen is longer than it was originally, and the surrounding elastic material is trying to compress it back to its original length. This puts the element in compression and is where the residual stress arises from. However, as the plastic strain decreases through anelastic recovery the mismatch is gradually reduced and not as great as at first. The surrounding material, consequently, does not exert as great a compressive stress as it did originally. The transient portion is given by

$$\sigma_{Rtrans} = (\sigma_{RO} - \sigma_{Req})\exp(-2.303\ t/t_{eq}) \tag{23}$$

This process was found by Bentley to be time dependent rather than cycle dependent. The anelastic recovery was measured on one specimen undergoing a single load cycle, which was then left to sit. It was then measured on a specimen which was cycled continuously. The anelastic recovery was the same in each case. The residual stress decay is a function of time and not cycles.

The total expression for residual stress is

$$\sigma_R = \sigma_{Req} + (\sigma_{RO} - \sigma_{Req})\exp(-2.303\ t/t_{eq}) \tag{24}$$

If σ_{Req} is expressed as a percentage of σ_{RO}, the anelastic recovery tests can be used to evaluate the unknown parameters in the model. The σ_{RO} is pro-

duced by the mismatch in the strains at the edge of the notch

$$\sigma_{RO} = k\ \varepsilon_p \tag{25}$$

The equilibrium stress, σ_{eq}, is produced by the mismatch in strains remaining after time.

$$\sigma_{Req} = k\ \varepsilon_{eq} = \sigma_{RO}\ \left(\frac{\varepsilon_{eq}}{\varepsilon_p}\right) \tag{26}$$

Using these in the expression for σ_R yields

$$\sigma_R = \sigma_{RO}\left[\left(\frac{\varepsilon_{eq}}{\varepsilon_p}\right) + \left(1 - \frac{\varepsilon_{eq}}{\varepsilon_p}\right) \exp\left(-\ 2.303\quad t/t_{eq}\right)\right] \tag{27}$$

Tests were run at two different strain levels in the plastic zone with results as given in the following table:

TABLE II

ε_p	ε_{eq}	$\varepsilon_{eq}/\varepsilon_p$	t_{eq}
.00540	.005033	.932	53.49 min
.005046	.004784	.948	50.05 min

A broader range of strain levels in the plastic zone would need to be run to determine if $\varepsilon_{eq}/\varepsilon_p$ is a constant and if t_{eq} is a material constant.

If this were the case, the residual stress expression would become

$$\sigma_R = \sigma_{RO}\ [0.94 - 0.06 \exp\ (-\ 0.0919t)] \tag{28}$$

where σ_{RO} is found as described in the last section.

Certainly these few tests cannot be relied upon to accept this expression as factual for 7075-T651; however two important points have been forthcoming. First, the stress decay was dependent upon time and not upon cycles, and secondly it was small in magnitude. All of this will be probed more thoroughly and deeply during the next year.

V. SUMMARY AND CONCLUSIONS

A fatigue monitoring instrument based upon a microcomputer has been demonstrated in laboratory and preliminary flight test to be feasible and very desirable. Due to its adoption for future aircraft by NAVAIR, investigations have been begun for effective use of the far-field strain data recorded by it to compute fatigue damage.

Three major areas have been undertaken in this study: (1) A sophisticated computer program has been used to investigate the effects of the minimum portion of each load cycle on the accumulated fatigue damage. (2) Analytical and experimental investigations have been made of the use of Neuber's equation in calculating local stress from far-field strain with the result that a better equation was developed. (3) An experimental investigation of the relaxation of residual stresses produced at sites of stress concentration was undertaken with some success but with other work to be done before these results are conclusive.

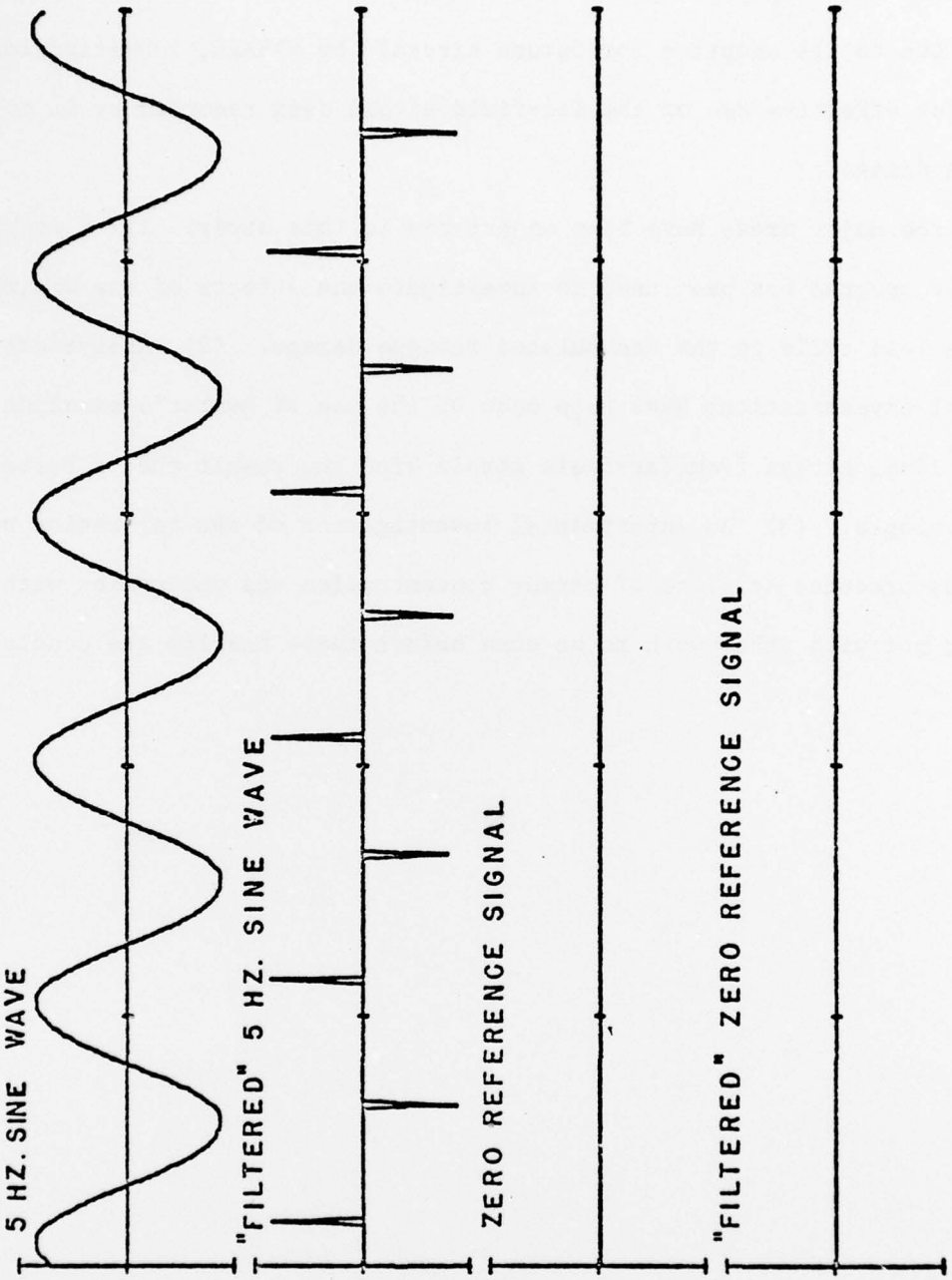

Figure 1 Laboratory Test Results of the Fatigue Monitor

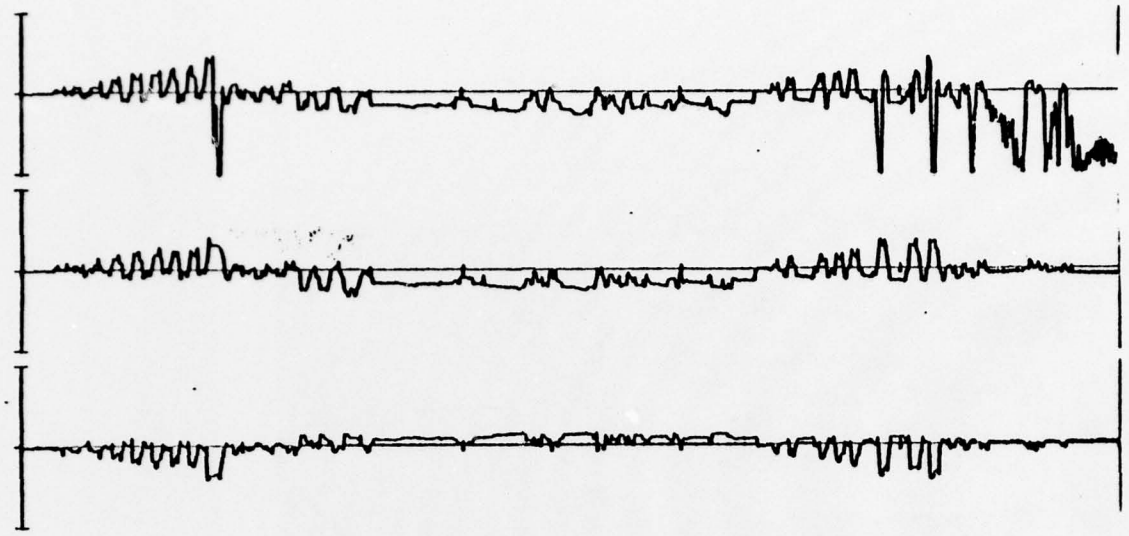

Figure 2. Example flight trace of 3 channels from MIDAS I

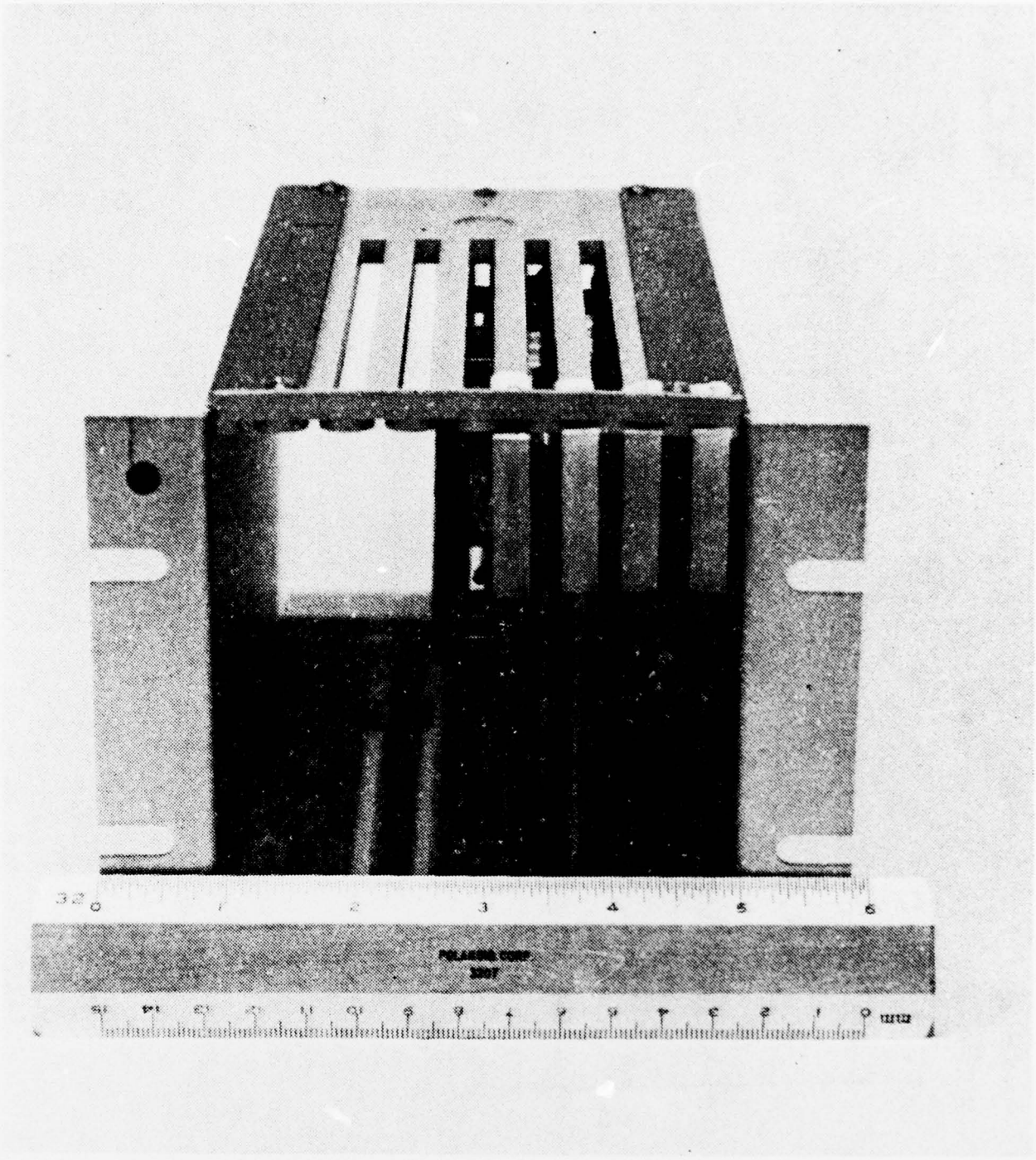

Figure 3 MIDAS Aircraft Fatigue Monitor

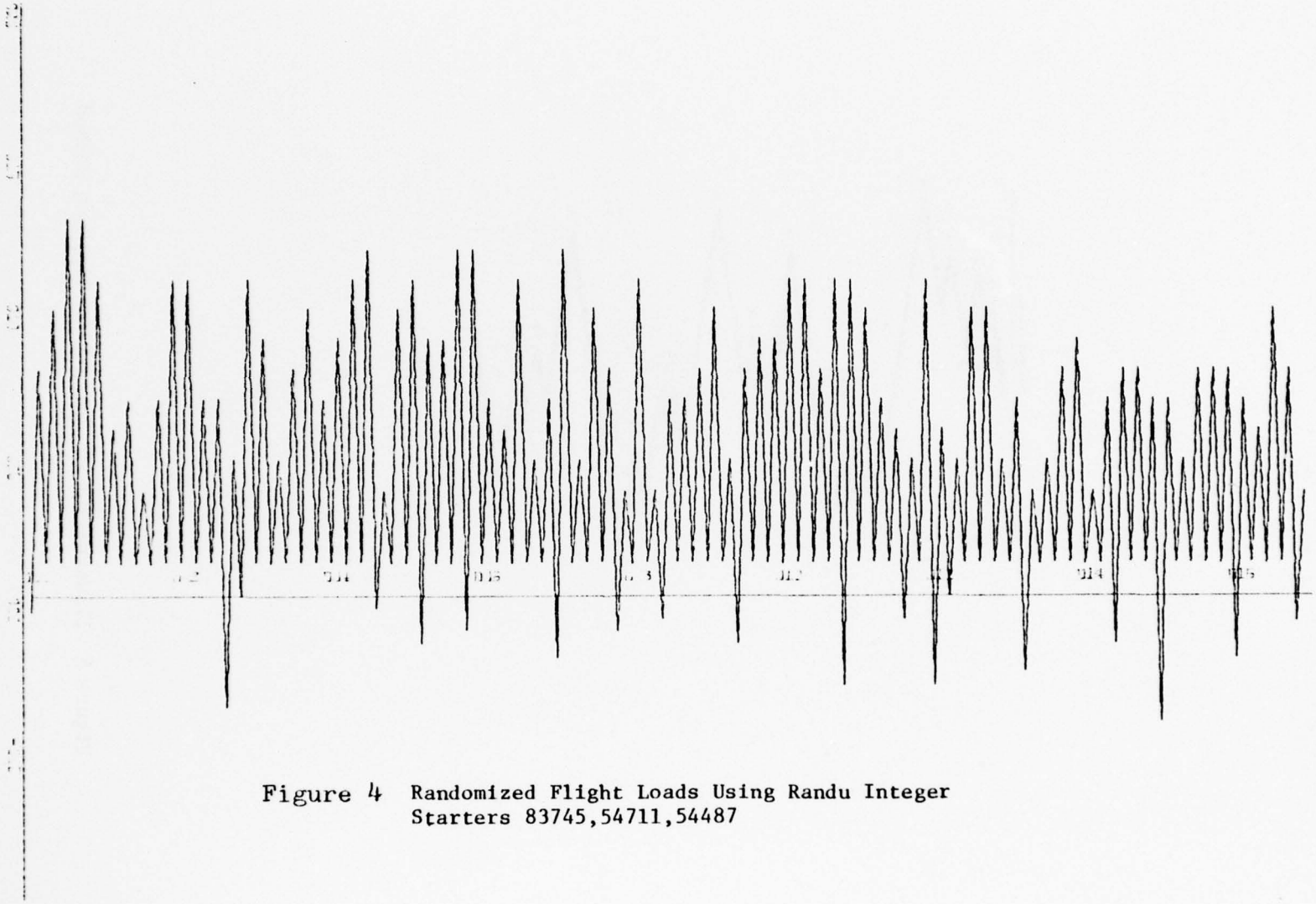

Figure 4 Randomized Flight Loads Using Randu Integer Starters 83745,54711,54487

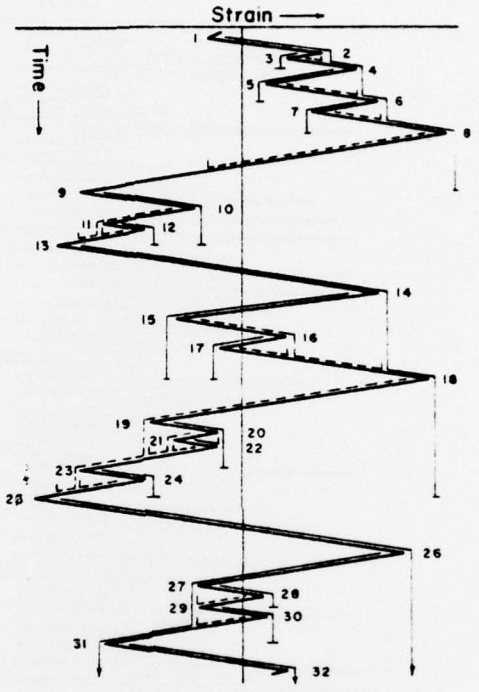

Figure 5 Illustration of Range-Pair Counting Method

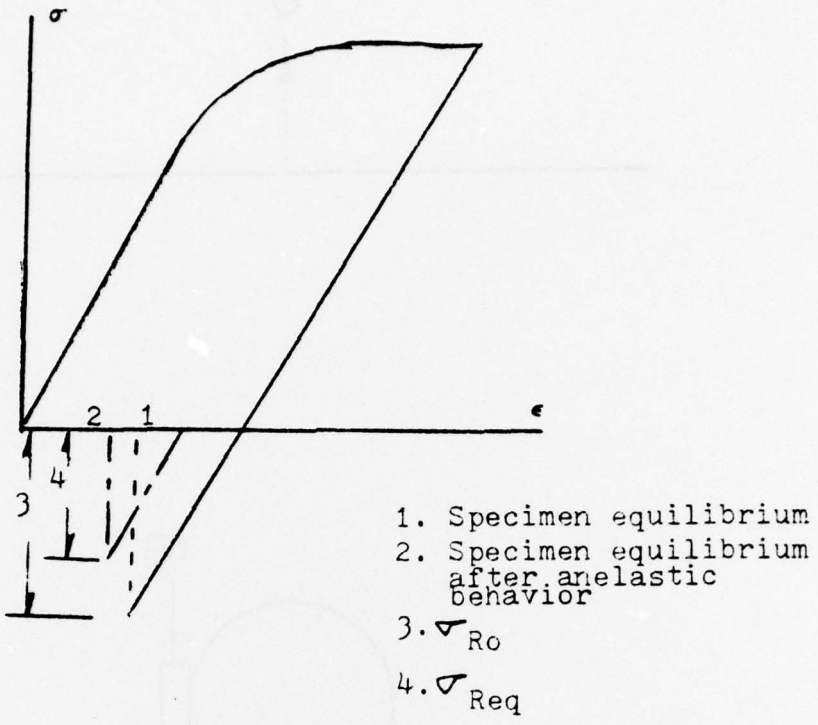

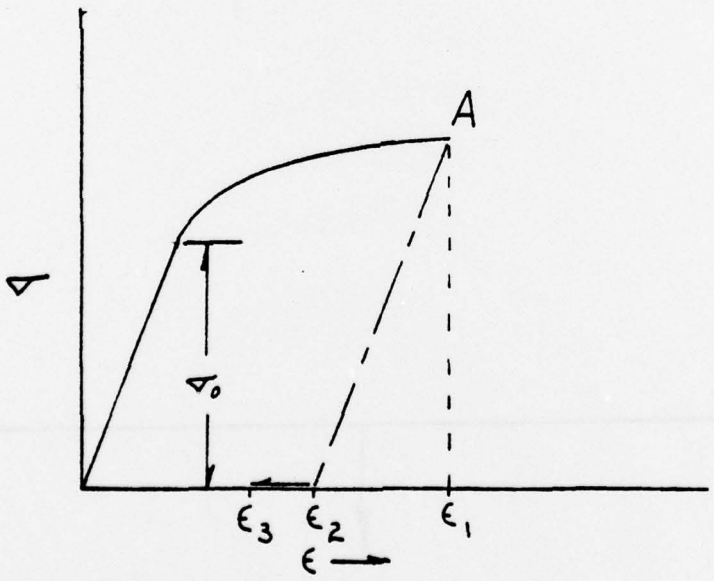

Figure 6 An Illustration of Anelastic Behavior

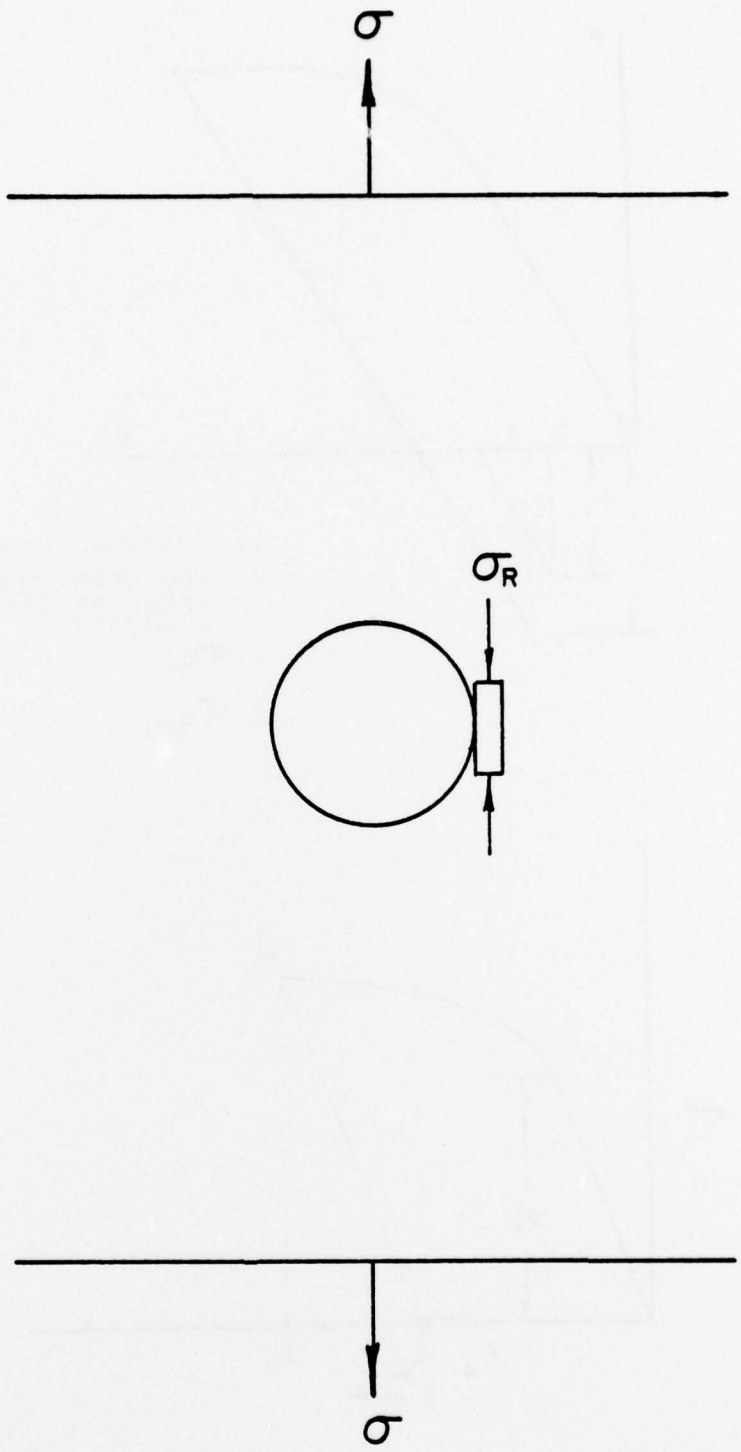

Figure 7 Uniaxial Representation of Residual Stress

VI. REFERENCES

1. David M. Vidrine, "A Sequential Strain Monitor and Recorder for Use in Aircraft Fatigue Life Prediction", Master's Thesis, Naval Postgraduate School, June 1975.
2. J. W. Sturges, "A Microprogrammable Data Acqusition System", Engineer's Thesis, Naval Postgraduate School, June 1975.
3. W. C. Stanfield, "Microprogrammable Integrated Data Acquisition System: Fatigue Life Data Application", Master's Thesis, Naval Postgraduate School, March 1976.
4. C. Lynn Butler, "Software Design for a Fatigue Monitoring Data Acquisition System", Master Thesis, Naval Postgraduate School, September 1976.
5. J. M. Potter and R. A. Noble, "A User's Manual for the Sequence Accountable Fatigue Analysis Computer Program", AFFDL-TR-23, May 1974.
6. R. M. Engle, Jr., "Cracks II User's Manual", AFFDL-TM-74-173, Air Force Flight Dynamics Laboratory, July 1974.
7. J. Scott Atkinson, "A Study of Spectrum Loading and Range - Pair Counting Method Effects on Cumulative Fatigue Damage", Master's Thesis, Naval Postgraduate School, March 1977.
8. J. W. Darnell, Jr. and J. N. Cherry, "A-7 Wing Fatigue Life", Vought Aeronautics Division Report No. 2-53420/OR-5562, August 1970.
9. G. M. van Dijk, "Statistical Load Data Processing", 6th International Conference on Aeronautical Fatigue Symposium, May 1971.
10. J. M. Potter, "The Effect of Load Interaction and Sequence on the Fatigue Behavior of Notched Coupons", ASTM STP519, 1973.
11. C. E. Inglis, "Stresses in a Plate Due to the Presence of Cracks and Sharp Corners", Proc. Inst. of Naval Architects, March 1913.

12. H. J. Neuber, "Theory of Stress Concentration for Shear-Strained Prismatical Bodies with Arbitrary Nonlinear Stress—Strain Law", Trans. ASME Journal of Applied Mechanics, Vol 8, Dec 1961, p. 544.

13. John C. Garske, "An Investigation of Methods for Determining Notch Root Stress from Far-Field Strain in Notched Flat Plates", Master's Thesis, Naval Postgraduate School, September 1977.

14. Richard A. Bentley, "An Investigation of the Recovery Processes in 7075-T651 Aluminum Responsible for a Stress Decay Suring Dynamic Loading Histories", Master's Thesis, March 1977.

VII. DISTRIBUTION LIST

		No. of Copies
1.	Defense Documentation Center Cameron Station Alexandria, VA 22314	2
2.	Library, Code 0142 Naval Postgraduate School Monterey, CA 93940	2
3.	Dean of Research Code 012 Naval Postgraduate School Monterey, CA 93940	1
4.	Department of Aeronautics Code 67 Naval Postgraduate School Monterey, CA 93940	
	Professor R. W. Bell, Chairman	2
	Associate Professor G. H. Lindsey	5
5.	Dr. Al Sommaroff Code 320B Naval Air Systems Command Washington, DC 20361	2
6.	Dr. Ed McQuillen Head Structures Branch Naval Air Development Center Warminster, PA 18974	1